Energy Transfer in the Restricted Geometry of Lamellar Block Copolymer Interfaces

J. P. S. Farinha‡

Centro de Química-Física Molecular, Instituto Superior Técnico, Av. Rovisco Pais, 1049-001 Lisboa, Portugal

John G. Spiro† **and M. A. Winnik***

Department of Chemistry, University of Toronto, 80 St. George Street, Toronto, Ontario, Canada M5S 3H6

Received: June 30, 2000; In Final Form: February 21, 2001

We carried out simulations of energy transfer kinetics for lamellar block copolymer systems in which donor and acceptor dyes were attached to the block junctions. We considered blocks of homopolymers that were sufficiently immiscible and of sufficiently high molecular weight to employ the Helfand−Tagami distribution of block junctions. The morphology of such block copolymers has been frequently discussed in terms of an apparent dimension parameter, which is recovered from the analysis of fluorescence decay curves, using the Klafter−Blumen (KB) formalism. Here, we investigate how such apparent dimensions are influenced by the interface thickness between the two blocks (which is dependent on the Flory−Huggins χ parameter of the system). We also probe the dependence of this apparent dimension on the concentration of the dyes in labeled samples. This kind of dependence has been experimentally observed but never explained, perhaps because of the approximations inherent in using the KB model to analyze fluorescent decay curves for block copolymer systems. We have found that apparent dimensions approach three for reasonably broad interfaces, but decrease to near two for very narrow interfaces, in accordance with asymptotic formulas that we propose for strongly segregated, lamellar block copolymer melts. Global analysis of the decay curves, as well as weighted linear regression of the parameters obtained from individual analyses of the decays, suggest linear relationships between the apparent dimensions from KB analyses and acceptor concentrations. We discuss the dependence on interface thickness in terms of the basic (Förster) theory of direct energy transfer, and indicate why the KB model is a reasonable representation of lamellar block copolymers.

Introduction

The characteristic feature of most polymer mixtures is that the components do not mix on a macroscopic scale. Binary blends of most homopolymers not only form separate phases, but the sizes of the domains often depend on the processing history of the sample.[1] If one or both of the components are rigid glasses at room temperature, then the morphology generated during processing is frozen in the material. Diblock copolymers represent a special case of a system composed of two polymer components attached at a common junction. If the polymer molecules are similar in length and composition, and the two components have limited miscibility, then the components will form separate phases. The degree of phase separation is limited by the covalent bond between the two polymers, and in order to satisfy the space-filling requirements of uniform density, such systems self-assemble into periodic structures. If the two polymers are approximately the same length, a periodic lamellar structure is formed.[2−4]

One of the most interesting topics in contemporary polymer science involves the characterization of the interface between polymer domains. These interfaces are important because the macroscopic mechanical properties of the material depend on the adhesion and the transfer of stresses across the interface, as for example, in impact modified plastics. Unlike inorganic materials where interfaces are sharp and characterized by thicknesses of at most a few angstroms, polymer−polymer interfaces are by comparison more diffuse. In the few instances where reliable data are available, values ranging from 2 to 8 nm are found.

The theoretical description of polymer interfaces begins with consideration of the Flory χ parameter, which describes the free energy of interaction between the repeat units of the two polymers. While χ has a value larger than zero in immiscible blends, the values are often small. In these situations a significant extent of segment interpenetration occurs between the two components at the domain interface. The theory of block copolymer interfaces reveals that block copolymer interfaces and polymer blend interfaces share many common features. The major difference in the free energy of interface formation is the entropy penalty for localization of the joints in the interface for block copolymers. This term becomes smaller as the polymers become longer, and for long chains, the interface thicknesses are predicted to be the same in both systems.

Over the past decade there have been major advances in our ability to study polymer interfaces. The most powerful technique is neutron reflectivity (NR), in which one observes the specular reflection between thin films of the two polymers. To have contrast, selective deuteration of one of the polymer components is necessary.[4−7] This is an important technique for the study of both blends and self-assembling block copolymers, but is limited to the lamellar geometry. Small-angle neutron scattering (SANS) and small-angle X-ray scattering (SAXS) experiments are both

* To whom correspondence may be addressed. E-mail: mwinnik@chem.utoronto.ca.
† E-mail: jspiro@chem.utoronto.ca.
‡ E-mail: farinha@ist.utl.pt.

10.1021/jp002345+ CCC: $20.00
Published on Web 05/09/2001

sensitive to the sharpness or diffuseness of the interface between components of different contrast factors, but the interpretation of the data is not as rigorous as in the case of NR. Here one looks for deviations from Porod-Law scattering in a region where the scattering intensity is weak. Both NR and scattering techniques are sensitive to other factors such as waviness at the interface, which increase the apparent diffuseness of the interface, and the data require appropriate corrections.[8]

An alternative approach to studying polymer interfaces is nonradiative energy transfer (ET) experiments, employing fluorescent labels ("dyes") attached to the two components, at very low concentrations. The number of groups actively employing this technique has been small. Fredrickson was first to point out the utility of this type of experiment for junction labeled block copolymers.[9] If one mixes block copolymers, one labeled with an energy donor dye and the other with an energy acceptor dye, phase separation leads to confinement of the dyes in the interface, with a consequent increase of the quantum efficiency of energy transfer between the dyes. The kinetics of ET between the donors and acceptors will also be very sensitive to the donor−acceptor distance distribution, which in turn depends on the distribution of the polymer junction points in the interface. Thus, energy transfer determinations can provide information on how sharp or diffuse the interface is. However, actual experimentation with specifically labeled block copolymers needed to wait, until particular synthetic difficulties were overcome.[10,11]

For this tool to be employed properly, we need an appropriate theory of energy transfer in the restricted dimensions of the interface. A starting point is Förster's expression for the rate of energy transfer in dipole−dipole interactions:[12,13]

$$w(r) = \frac{3}{2}\frac{\kappa^2}{\tau_D}(R_0/r)^6 \tag{1}$$

where τ_D is the donor lifetime in the absence of acceptors and r is the distance separating the donor−acceptor pair. The constant κ^2 is a dimensionless transition-moment orientation-factor, which we have assumed to be approximately 0.47 in this work,[14] and R_0 is the Förster radius, which may be calculated from spectroscopic data.

A major advance in applying Förster's relationship to systems of restricted geometry was due to Klafter and Blumen, who derived the relationship[15]

$$\Phi(t) = \exp\left(-\frac{t}{\tau_D}\right)\exp\left[-P\left(\frac{t}{\tau_D}\right)^{\beta}\right] \tag{2}$$

as a general description of the survival probability $\Phi(t)$ for excited donors in infinite media of any dimensionality. The above eq 2, with $\beta = d/6$, generalizes expressions derived by Förster for direct energy transfer (DET) in three dimensions ($d = 3$),[12−14] and by Hauser and co-workers for one ($d = 1$) and two ($d = 2$) dimensions.[16] Klafter and Blumen showed that, for donors and acceptors embedded in a fractal lattice, d is equal to the fractal dimensions of the lattice. Fractals are characterized by self-similarity over a variety of length scales. In fractal structures, the parameter $d = 6\beta$ in eq 2, corresponds to the fractal (Hausdorff) dimensionality of the lattice on which the dyes are distributed. The parameter P is proportional to the local concentration of acceptors.

Subsequently, Klafter, Blumen and Zumofen[17] found that this type of formalism could be applied to DET in systems of restricted geometry. The term "restricted geometry" refers to a space or domain confining the dyes in which at least one dimension is on the order of R_0 in size. In a restricted geometry, the fractional value β is due to edge effects of the confining space. For the latter systems, the value 6β is sometimes referred to as the "apparent dimensionality".[18] The KB eq 2 and similar formulas have been applied to a variety of systems, such as porous solids,[19] surfactant vesicles,[20] and in the simulation of regular lattices with excluded volume.[18]

It was probably El-Sayed and co-workers who first reported the utility of eq 2 for determining the apparent dimension of structures that are clearly not of a fractal nature.[18] Although the application of eq 2 to systems of restricted geometry is strictly empirical in most cases, the apparent dimension parameter obtained from this equation can give some information on the nature of the domains where donor and acceptor dyes are distributed. This was recently shown for the case of poly(isoprene-*b*-methyl methacrylate) [PI−PMMA] block copolymer micelles in acetonitrile, where a relationship between this apparent dimension and the thickness of the interfacial domain between the core and corona of the micelles was found.[21]

In some systems of restricted geometry, constant "apparent dimension"[18] will be obtained within the range of experimental parameters available to the experimentalist. On other occasions, however, eq 2 can be fitted to experimental data only over a limited range of decay times and/or acceptor concentrations, resulting in so-called crossover effects in the value of the exponent $\beta = d/6$ recovered from analyzing the data. Indeed, the impetus for the work reported here came from such crossover effects that we had found for solid films of PI−PMMA, as a function of the donor-to-acceptor ratio.[22] It seemed useful to acquire a better understanding of the apparent dimensions found in DET experiments on lamellar block copolymer systems.

The basic concepts of Klafter and Blumen's derivations are embodied in the survival probability formula

$$\Phi(t) = \exp(-t/\tau_D)\psi(r_0,t) \tag{3a}$$

$$\psi(r_0,t) = \exp(-p\int_V\{1 - \exp[-tw(r)]\}s(r)\mathrm{d}V) \tag{3b}$$

where t is time after excitation and r_0 is the position of the donor with respect to some appropriate coordinate system. The distribution of acceptor molecules around each donor is described by the parameters p and $s(r)$, p being the probability that an allowed occupation site is actually filled by an acceptor species, and $s(r)$ the distribution function that describes the separation of donor−acceptor pairs. The latter function may be difficult to obtain in the most general situation, but in recent years our group has developed a theoretical methodology for computing the survival probabilities whenever the donor and acceptor concentration profiles follow an element of symmetry: planar[23,24] or spherical.[25,26] Specifically, for planar geometry one obtains the expression

$$\Phi(t) = \exp\{-t/\tau_D\}\int_{-\infty}^{+\infty}C_D(z)\psi(z,t)\mathrm{d}z \tag{4a}$$

$$\psi(z,t) = \exp\{-g(z,t)\} \tag{4b}$$

$$g(z,t) = 4\pi\int_0^{\infty}[1 - \exp\{-w(r)t\}]\langle C_A(z,r)\rangle r^2\,\mathrm{d}r \tag{4c}$$

$$\langle C_A(z,r)\rangle = \frac{1}{2r}\int_{z-r}^{z+r}C_A(z')\mathrm{d}z' \tag{4d}$$

In eq 4a, z represents the axis along which concentration profiles vary. Because the intensity is measured in arbitrary units, we

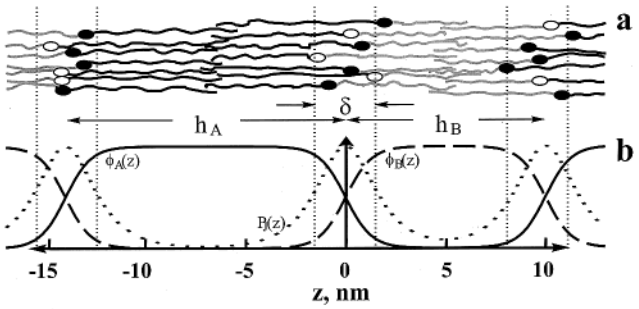

Figure 1. (a) Schematic representation of the microphase separation of A−B diblock copolymer chains into a lamellar morphology. Since each junction point is labeled by either of a donor (○) or acceptor (●) dye, the dyes concentrate at the interface. (b) Example of calculated profiles of block volume fractions (ϕ_A and ϕ_B) and the junction distribution function ($P_J(z)$) across a section of the film, using the Helfand−Tagami relations, with parameters approximating the case of PI−PMMA, cf. Table 1: Period spacing length $H = h_A + h_B = 24$ nm and interface thickness $\delta = 2.6$ nm.

have omitted all proportionality constants of eq 4a. The function $\psi(z, t)$ measures the probability that an excited donor, positioned on a plane at z, "survives" for a time t before energy transfer occurs. The exponent function $g(z, t)$ and the mean acceptor concentration $\langle C_A(z,r)\rangle$ are defined to simplify the presentation. Physically, $4\pi r^2\, dr\, \langle C_A(z,r)\rangle$ may be interpreted as the mean number of acceptors within a shell of radius r and thickness dr surrounding a donor positioned on a plane at z. In eq 4d the profile $C_A(z')$ must be in units of number density. To calculate $\Phi(t)$, the information needed is the spatial dependence of concentration profiles $C_D(z)$ and $C_A(z)$, features determined by the local morphology of the system.

We will assume that Helfand and Tagami's junction distribution function[27] may be employed to describe the interface morphology of equilibrium microphase-separated A−B block copolymers:

$$P_J(z) = \frac{(2/\pi)}{\delta}\mathrm{sech}(2z/\delta) \tag{5}$$

$$\delta = \frac{2b}{\sqrt{6\chi}} \tag{6}$$

where $P_J(z)\, dz$ represents the probability of finding a junction point between z and $z + dz$, δ is the interface thickness, b is the statistical segment length, and χ is the Flory−Huggins parameter. From eq 5 one can define normalized acceptor and donor distribution functions:[28]

$$C_A(z) = \frac{H\bar{C}_A}{2}P_J(z) \tag{7a}$$

$$C_D(z) = \frac{H\bar{C}_D}{2}P_J(z) \tag{7b}$$

where $\bar{C}_\alpha$ (α = A, D) are the bulk-averaged, experimentally determinable, dye concentrations in the sample. In actual practice, one needs to know only $\overline{C_A}$ (in units of number density). Knowledge of $\bar{C}_D$ is not necessary because, as indicated in eq 4a, intensity measurements are made in arbitrary units. H is the lamellar period, as illustrated in Figure 1.

We have previously reported[28] that for very narrow interfaces (in the limit $\delta = 0$), eqs 4 and 7 lead to a donor survival probability formula similar to Hauser and co-workers' result for an isotropic mixture of donors and acceptors on an infinite, two-dimensional surface.[16] Here, we show (Appendix A) that for very broad interfaces the asymptotic ($\delta \to \infty$) formula suggests three for the apparent dimensionality of the block copolymer junction. For interfaces of intermediate thickness, one would then hope to be able to fit the experimental or simulated data to the KB eq 2, and find intermediate d values, i.e., d between two and three ($^1/_3 < \beta \equiv d/6 < {}^1/_2$). We will examine the validity of this conjecture, and how it agrees with data obtained from experimental studies.

TABLE 1: Block Copolymer Characteristics

input parameters	block copolymer samples: PS−PMMA[10]	PI−PMMA[11,21]
period spacing H, nm	34.5	27.0
interface thickness δ, nm	5.17	2.60
film Förster radius R_0*, nm	2.17	2.17
donor lifetime τ_D, ns	44	45

Simulation of Data

The computations and discussion are based on experimental data earlier obtained for poly(styrene-*b*-methyl methacrylate) [PS−PMMA] and poly(isoprene-*b*-methyl methacrylate) [PI−PMMA] films, where the polymer chains are organized in lamellar domains. A cartoon of the film morphology, also showing labeling at the junctions, is presented in Figure 1; the properties of the block copolymers are shown in Table 1. We previously reported the characterization of these block copolymers, including apparent dimensions from fitting fluorescence decay data to eq 2.[10,11,22] The simulation techniques have also been described,[28] except that this time we did not introduce a light scattering contribution to the data for any of the simulated experiments. To examine more closely the influence of junction thickness, we also carried out simulations for a hypothetical, narrow-interface ($\delta = 1.0$ nm) block copolymer, with a lamellar period the same as that of our PI−PMMA sample (27 nm). Such narrow interfaces have been found in PI−PMMA block copolymer micelles in a solvent selective for PMMA. [21]

As mentioned in the Introduction, crossover effects may arise if one fits eq 2 to fluorescence decay measurements on samples containing different acceptor concentrations. To study such effects, we conducted simulations (and subsequent analyses of the simulated data) over rather broad ranges of the bulk acceptor concentration $\overline{C_A}$.

For each interface thickness we first simulated delta-function excitation fluorescence decay curves corresponding to different bulk acceptor concentrations $\overline{C_A}$. Each of these decays was then convoluted[28] with the same experimental lamp profile, and finally three replicate fluorescence curves were obtained by adding Poisson noise.

Analysis of the Simulated Data

We fitted the simulated data to eq 2 as if they had been experimental decays. Figure 2 shows an example of the analysis of simulated decay curves, here for the PI−PMMA block copolymer (Table 1) and an acceptor concentration of 1.8×10^{-5} mol/cm^3. Equation 2 seemed a good representation of the "data" here, with randomly distributed weighted residuals and autocorrelation of the residuals.

Details of the *basic* procedures have been published,[28] but here we were dealing with *series* of simulated samples, representing different acceptor concentrations. Let us first consider the dependence of the P parameter of eq 2 on the

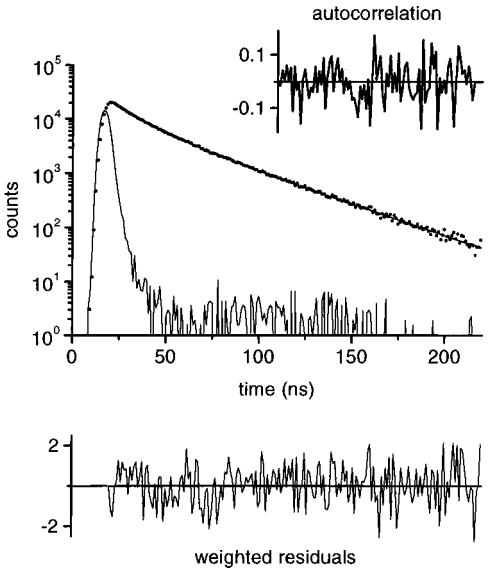

Figure 2. Analysis of a fluorescence decay curve simulated for the junction-labeled PI−PMMA block copolymer sample, at relatively low acceptor concentration (1.8×10^{-5} mol/cm^3). A Helfand−Tagami distribution of junctions, with the parameters shown in Table 1, was assumed in the simulation; the intensities obtained were fitted with eq 2.

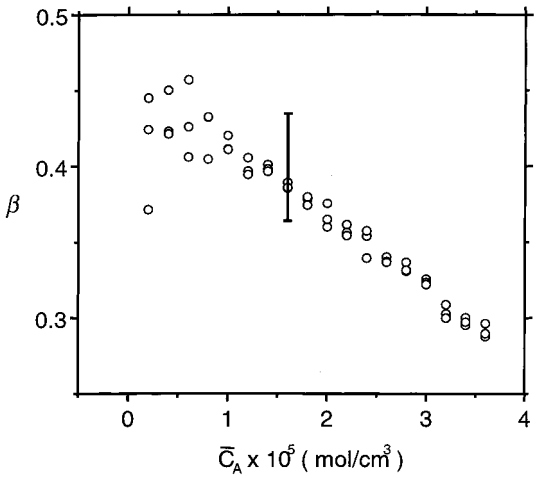

Figure 3. Linear relationship between the parameter β of eq 2 and the acceptor concentration. The β parameter values were recovered by fitting fluorescence decay curves simulated using the PI−PMMA parameters (Table 1) with eq 2. The error bar shown indicates the estimated uncertainty of β, if determined only at a single concentration; the large uncertainty derives from the very shallow χ^2 surfaces for the individual fittings. Although not evident from the figure, we found that the autocorrelation plots and χ^2 values show increasingly serious fitting difficulties at acceptor concentrations exceeding 2.5×10^{-5} mol/cm^3.

acceptor concentration. For fractal structures, Even and coworkers[29] suggested that the P parameter in eq 2 is given by

$$P = x_A(D/d)\Gamma(1-\beta)(R_0/a)^d \qquad (8)$$

where x_A is the fraction of fractal sites occupied by the acceptors ($x_A \ll 1$), D is the dimension of the embedding Euclidean space, Γ is the complete gamma function, and a is the average size of a unit cell. For lamellar block copolymers, a different expression was proposed earlier[10,22]

$$P = (4\pi R_0^3 N_{Av} R/3\delta V_B) g^\beta \Gamma(1-\beta)\overline{C_A} \qquad (9)$$

where N_{Av} is Avogadro's number, R and V_B are the half-length and volume fraction, respectively, of the minor phase, and g is an orientation factor. Both eqs 8 and 9 suggest that when all other conditions remain unchanged, P will be proportional to the acceptor concentration. Indeed, we routinely employ this test to detect errors, artifacts or other difficulties in our experimental data. The formulas also indicate, however, that should the exponent β of eq 2 change in a series of experiments, then the simple relationship between $\overline{C_A}$ and P may break down. Nevertheless, in some of our experimental work the $P = k_1 \overline{C_A}$ proportionality persisted well into the range of acceptor concentrations where β was changing rapidly,[22] and analyses of the simulated decay curves of the present paper also suggested that it was reasonable to assume such a relationship.

Whereas eqs 8 and 9 provide a certain guidance as to what to expect in terms of the P prefactors obtainable by the analyses with eq 2 of experimental or simulated fluorescence decay curves corresponding to lamellar block copolymers, the variation of the β values is more difficult to interpret. The asymptotic results mentioned in the Introduction suggest that one should obtain low (not much higher than $^1/_3$) β values for narrow interfaces, and higher (approaching $^1/_2$) values for broad junctions. This is very vague information, and it is even more difficult to predict how the acceptor concentrations will affect β. However, at an early stage of the present work, we found a very pronounced affine relationship between the exponent β and the bulk acceptor concentration (Figure 3). Figure 3 suggests that this relationship is valid even for high acceptor concentrations, when the KB model no longer represents the data adequately ($\overline{C_A} > 2.5 \times 10^{-5}$ mol/cm^3). The latter limitation of the KB model is easily detectable by the increasingly nonrandom nature of the Grinvald-Steinberg[30] autocorrelation plots, as in Figure 4, as well as by the deterioration of the χ^2 values of the fits. Figure 4 shows the analysis of a simulated decay curve for the PI−PMMA block copolymer (Table 1) at an acceptor concentration of 3.2×10^{-5} mol/cm^3. The χ^2 value

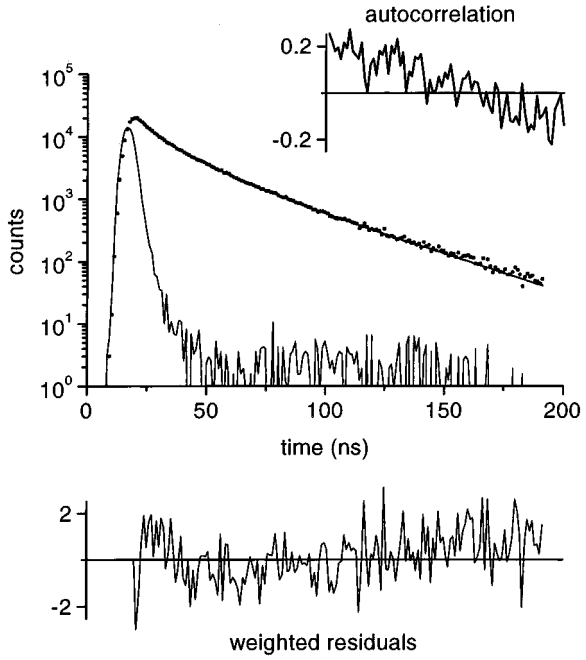

Figure 4. Analysis of a fluorescence decay curve simulated for the junction-labeled PI−PMMA block copolymer sample (model parameters as in Table 1), at high acceptor concentration (3.2×10^{-5} mol/cm^3). The fluorescence decay curve was fitted with eq 2. Here, the fit is definitely flawed.

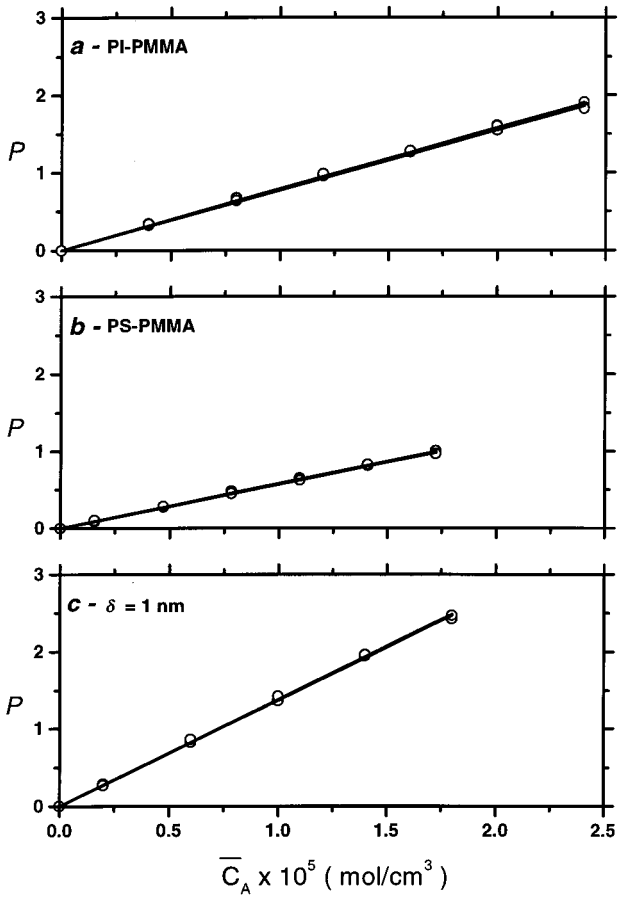

Figure 5. Linear relations between acceptor concentrations and the *P* factors recovered from the KB fit (eq 2) of fluorescence decay curves simulated for (a) the PI−PMMA interface, $\delta = 2.60$ nm; (b) the PS−PMMA interface, $\delta = 5.17$ nm; and (c) the narrow interface, $\delta = 1.0$ nm. Each straight line seen is actually a pair of straight lines, indistinguishable at this resolution. One of them shows the weighted linear regression of *P* parameters obtained from individual fits of the decay curves; the other one represents the results of global analysis.

obtained was 1.26, acceptable in itself, but the nonrandom autocorrelation plot clearly rejects the KB model.

Despite the uncertainties, the preceding discussion does suggest a phenomenological reparametrization of eq 2:

$$\Phi(t) = \exp\left[-\frac{t}{\tau_D} - k_1\overline{C_A}\left(\frac{t}{\tau_D}\right)^{\beta_0 + k_2\overline{C_A}}\right] \qquad (10)$$

with k_1, β_0, and k_2 constant for a given block copolymer. In turn, eq 10 suggests a global analysis approach,[31] which was also necessitated by the fact that the χ^2 surfaces for individual decay curves were very shallow. The error bar in Figure 3 indicates our estimate of the lack of precision we would have to accept without resorting to at least a simple type of global analysis.

Results and Discussion

We will now present the outcome of the KB (eq 2) analyses of the three sets of simulated fluorescence decay curves, representing lamellar block copolymers with junction thicknesses of $\delta = 5.17$ nm, $\delta = 2.6$ nm, and $\delta = 1.0$ nm, and different bulk acceptor concentrations. From these analyses we recovered the parameters *P* and β.

In Figure 5 we present the values obtained for the *P* parameter. For each of the three sets of simulated curves we found the usual proportionality between *P* and the bulk acceptor concentration $\overline{C_A}$. The results of the weighted linear regressions of *P* vs $\overline{C_A}$ are shown in Table 2 as well—here in terms of the k_1 parameter of eq 10. (Weights were conveniently defined via the standard errors of the model parameters *P* and β, as estimated by the nonlinear least-squares fitting program).[28,32,33]

In Figure 6 we show the weighted linear regression lines approximating the β versus $\overline{C_A}$ points. For each of the three sets of simulated curves ($\delta = 5.17$, 2.6, and 1.0 nm) the relation between β ($\equiv d/6$) and the bulk acceptor concentration $\overline{C_A}$ is reasonably linear, although for the hypothetical, $\delta = 1.0$ nm block copolymer, the apparent dimension is best considered constant. (This is indicated in Figure 6; also see the discussion below.) To our knowledge, this type of dependence of the apparent dimensions on the acceptor concentrations has never been reported, nor predicted. Results of the weighted linear regressions of β are also shown in Table 2, again, with reference to eq 10.

To confirm the apparent straight-line dependencies of both *P* and β on $\overline{C_A}$, we conducted simple global analyses. Whereas global analysis ideally takes into account information from different kinds of experiments,[31] here we contented ourselves with fitting eq 10 to a *set* of simulated decay curves for any particular block copolymer. That is, k_1, β_0, and k_2 in eq 10 were determined by least squares from the entire set of simulated decay curves for a particular block copolymer, representing thousands of channels of "measured" fluorescence intensities. Some details of our global analysis methodology are given in Appendix B.

For the parameter *P*, the global analysis results are virtually identical to the results produced by the weighted linear regression analyses of values obtained from the individual decay curves (Table 2 and Figure 5). The assumed proportionalities between *P* and $\overline{C_A}$ are quite closely satisfied.

Figure 6 provides a certain amount of insight into how the fitting parameter β of eq 2 depends on the junction width and acceptor concentration for each interface thickness simulated. First, it is clear that whereas the $\beta = \beta_0 + k_2\overline{C_A}$ relationships hold fairly well for each block copolymer, the individual parameters, especially k_2, cannot be determined precisely (Table 2). Despite minor discrepancies between the weighted linear regression and global analysis results, the $d_0 \equiv 6\beta_0$ values are quite well defined, and are consistent with the asymptotic limits for very broad interfaces, $\delta \rightarrow \infty$ (see Appendix A), and very thin interfaces, $\delta \rightarrow 0$.[28] The parameter d_0 is quite close to 2 for the thin ($\delta = 1$ nm) interface simulated, which approaches a two-dimensional surface, and closer to 3 for the broader interfaces ($\delta = 2.6$ nm and $\delta = 5.17$ nm). Thus, it appears that the junction distributions of "ordinary" block copolymers are already broad enough to yield apparent dimensions approaching three in time-resolved fluorescence measurements of the type considered here (using eq 2 as a model and extrapolating the $\beta = d/6$ values obtained to zero acceptor concentration). Whereas an interface of thickness $\delta = 1.0$ nm is narrow enough to lead to an apparent dimension close to two, as also found experimentally for the case of PI−PMMA block copolymer micelles in acetonitrile.[21]

We should stress that the parameter d_0 is not a true spatial dimension, except in the extremes of a two-dimensional infinite surface ($d_0 = 2$) or a three-dimensional infinite volume ($d_0 = 3$). For all values in the range $2 < d_0 < 3$, the application of the KB formalism (eq 2) is strictly empirical,[21] and d_0 is thought to express the confining effects of the lamellar geometry.[18] We

TABLE 2: Apparent Block Copolymer Dimensions ($6\beta_0$) and Auxiliary Parameters (k_1 and k_2) Fitted to Equation 10

	weighted linear regression			global analysis		
block copolymer samples	$d_0 = 6\beta_0$	k_1 (nm^3)	k_2 (nm^3)	$d_0 = 6\beta_0$	k_1 (nm^3)	k_2 (nm^3)
PI−PMMA	2.72	131	−7.06	2.85	128	−8.06
PS−PMMA	2.88	96.1	−8.50	3.01	94.8	−10.2
$\delta = 1$ nm	2.21	229	−0.27	2.20	228	0.555

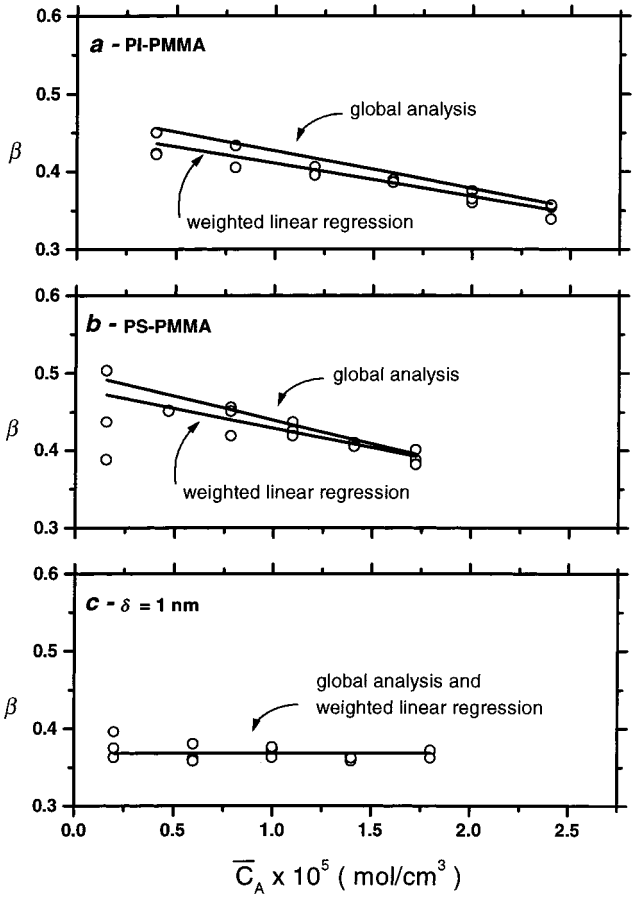

Figure 6. Linear relations between acceptor concentration and the β coefficient recovered from the KB fit (eq 2) of fluorescence decay curves simulated for (a) the PI−PMMA interface, $\delta = 2.60$ nm; (b) the PS−PMMA interface, $\delta = 5.17$ nm; and (c) the narrow interface, $\delta = 1.0$ nm. The pairs of straight lines represent the assumed $\beta = \beta_0 + k_2 \overline{C_A}$ relation (eq 10). As indicated, they were obtained from weighted linear regressions of the β coefficients from individual fits of the decay curves or by global analyses.

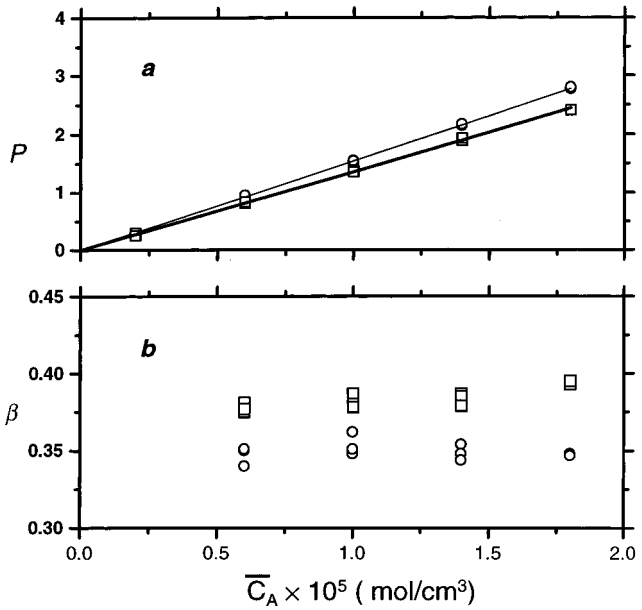

Figure 7. Analysis with eq 2 of simulated fluorescence decay curves obtained by assuming that the acceptors are distributed according to eqs 5 and 7a, but the donors have Dirac delta function distributions at $z = 0$ (the interface center) and $z = \delta$ (at a distance δ from the interface center). The simulations and analyses were carried out for the hypothetical, narrow-interface block copolymer ($\delta = 1.0$ nm, $H = 27$ nm). Please refer to Appendix C for further details. For off-centered donor molecules ($z = \delta$) we obtain higher β values from the fit ($\beta \approx 0.38-0.39$) than for donors placed at the center of the interface ($z = 0$), for which $\beta \approx 0.35$. (a) Plot of the P parameters recovered for donors at the center (○) of the interface ($z = 0$) and at a distance δ (□) from the interface center ($z = \delta$). (b) Plot of the β parameters recovered for donors at the center (○) of the interface ($z = 0$) and at a distance δ (□) from the interface center ($z = \delta$). We do not show the β values that were obtained at the lowest acceptor concentration (2×10^{-6} mol/cm^3), because their standard errors (as estimated by the nonlinear least-squares fitting program) were very high.

note from Figures 6a and b that the straight-line relationships implied by $\beta = \beta_0 + k_2 \overline{C_A}$ seem reasonable. For the narrowest interface simulated, the trend indicated by global analysis is directionally different from the regression results, although both approaches suggest that β does not depend strongly on $\overline{C_A}$ (Table 2). The most reasonable conclusion is that for the $\delta = 1.0$ nm simulations β should be regarded as a constant. In Figure 6c we plotted the horizontal line b $= \overline{\beta_0}$, where $\overline{\beta_0}$ was taken to be the average of the two β_0 values (from regression and global analysis).

The meaning of the parameter $d = 6\beta$ extrapolated to zero acceptor concentration, d_0, is a little vague. The apparent dimension d is a fitting parameter in a phenomenological equation; it should not be ascribed a direct physical meaning.[21] From our results, the apparent dimension extrapolated to zero acceptor concentration, d_0, appears to be the most significant fitting parameter. If we force the P and β values to obey the $P = k_1\overline{C_A}$ and $\beta = \beta_0 + k_2\overline{C_A}$ relationships, with the coefficients given in Table 2, we can obtain satisfactory analyses of the simulated decay curves at low acceptor concentrations. This procedure is much less successful at high acceptor concentrations, because of the uncertainty in the k_2 values.

The variation of the apparent dimension β with the acceptor concentration, found for results simulated with eq 4 and analyzed with eq 2, deserves a few more brief comments. While we believe that such variations are caused by the phenomenological nature of eq 2 when applied to the present systems, the decrease of β with increasing acceptor concentration can be interpreted in terms of the donor and acceptor distributions at the interface. To better understand this relationship, we simulated fluorescence decay curves for the case where the acceptors are distributed at the interface according to eqs 5 and 7a, but the donor molecules have Dirac delta function distributions at different positions: $z = 0$ (at the interface center) and $z = \delta$ (at a distance δ from the interface center). The decay functions obtained were again analyzed with eq 2, to recover the parameters P and β. In Figure 7 we present the outcome of these simulations. We observe that

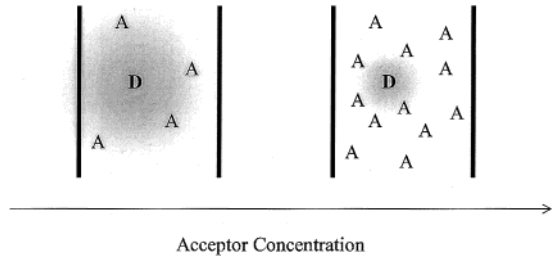

Figure 8. For a given donor, the probability that it will transfer energy to acceptors that are close is very high (the rate of energy transfer decreases with the inverse sixth power of the donor−acceptor distance). If the number of acceptors around this donor is increased, the donor will sense a smaller volume, because there will be energy transfer mainly to the closer acceptors. Therefore, the donors each probe a smaller volume (shown in shadow) at high acceptor concentration (right) than at low acceptor concentration (left). In the simulated system this shows up as a decrease in the apparent dimensionality with increasing acceptor concentration, when the decays are analyzed with eq 2.

for off-centered donor molecules ($z = \delta$) we obtain higher β values (Figure 7b, $\beta \approx 0.38-0.39$) than for donors placed at the center of the interface (Figure 7b; $z = 0$, $\beta \approx 0.35$).

It appears that when both donors and acceptors are distributed at the interface according to the Helfand−Tagami eq 5, energy transfer from donors positioned at the center part of the interface will produce smaller β values than from donors at the wings of the distribution.

Equation 1 states that the rate of energy transfer changes with the inverse sixth power of the distance between a donor and an acceptor. If we consider a given donor, the probability that it will transfer energy to acceptors that are close is very high. If the number of acceptors around this donor is increased, the donor will sense a smaller volume, because there will be energy transfer mainly to the closer acceptors. This is sketched in Figure 8.

When the interfacial region is thin compared to R_0, a change in the bulk acceptor concentration does not affect significantly the volume restriction imposed by the interface, because most of the acceptors are very close to the donor. This is the case of the copolymer simulated with a 1 nm interface, for which there is practically no dependence of the apparent dimension d on the acceptor concentration (Figure 6c).

On the other hand, if the interface thickness is large compared to R_0 (but still thin enough that edge effects are important), the donors can probe acceptor molecules that are farther. At high acceptor concentration the donors are more sensitive to the acceptors in the center part of the distribution, because most transfer occurs in this region (where most donors and acceptors are). Acceptors at larger distances from the center are "screened" from most of the donor molecules, by the large number of acceptors close by. This results in a lower β value because, as we learned from the simulation results shown in Figure 7, β is lower for transfer occurring to acceptors in the center of the interface than to acceptors in the wings of the distribution. At lower acceptor concentrations the donors are more sensitive to the acceptors in the wings of the distribution, which leads to higher β values. In summary, at low acceptor concentrations the donors probe more of the entire distribution. A good definition of the apparent dimension parameter extrapolated to zero acceptor concentration, d_0, appears to be a manifestation of such effects.

As discussed above, we conducted simulations with Dirac delta function donor distributions, to improve our understanding of the relationships between apparent dimensions (recovered by KB analyses) on the one hand, and the acceptor concentrations and interface thicknesses on the other. However, the simpler mathematical structure of the fluorescence decay functions arising from this approach (Appendix C) has also provided some insight into why the KB formalism (eq 2) is such a powerful tool for studying lamellar block copolymers, which are certainly not fractals. We note from Figure 7a that there is almost a strict proportionality between the P parameters recovered from the analyses in question and the acceptor concentrations; this has encouraged us to approximate the putative $P \alpha \overline{C_A}$ relationships by the slopes of the fitted straight lines. Strict adherence to KB theory would also require constant β values, independent of the acceptor concentrations. We have approximated the latter condition by replacing the beta values obtained in the individual analyses (for a given situation, such as donors at $z = 0$ only) by their averages over all acceptor concentrations.

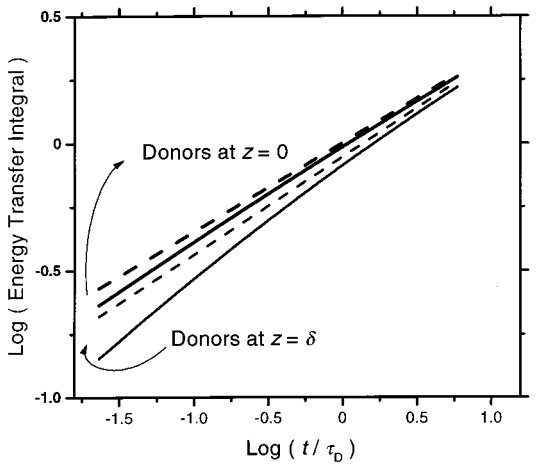

Figure 9. Log-log plots of the "energy transfer integrals" − the improper integrals shown in eqs C3a and C3b of Appendix C − for centered ($z = 0$) and off-center ($z = \delta$) donors, versus the reduced time (t/τ_D). The solid lines were calculated from the exact (within mean-field theory) formulas; the dashed lines correspond to the approximations obtained from the KB analyses (eq 2) of the simulated fluorescence decay curves. All results shown are for the hypothetical, narrow-interface block copolymer ($\delta = 1.0$ nm, $H = 27$ nm).

Let us now compare, for example, for the donors at the $z = 0$ case, the exact (within mean field theory) fluorescence decay function given in Appendix C, to eq 2. It will suffice to consider the negative logarithms of the *local* survival probabilities, the function *g(z,t)* of eq 4, here:

$$2H\overline{C_A}R_0^{*2}\int_0^\infty \left[1 - \exp\left(-\frac{t}{\tau_D}\rho^{-6}\right)\right]\left[2\arctan(e^{2R_0^*\rho/\delta}) - \frac{\pi}{2}\right]\rho\, d\rho \quad (11)$$

from the planar geometry approach [23,24] (where $R_0^* = (1.5\kappa^2)^{1/6}R_0$ is the Förster radius adjusted for the dipole orientation factor), and simply $P(t/\tau_D)^\beta$ from eq 2. We see that the KB model will be exact if the proportionality constant between $\overline{C_A}$ and P equals $2HR_0^{*2}$, and the improper integral in formula 11 is a straight-line function of t/τ_D in a log−log plot, with slope β and intercept zero.

Figure 9 shows that not only is the "required" linearity of the logarithms of the improper integrals quite closely satisfied, but the straight lines obtained from the somewhat crude estimates of the KB parameters are still reasonably close to the theoretical curves. This confirms the utility of eq 2 in fluorescence decay studies of lamellar block copolymer morphology.

In light of the foregoing results and discussion, it may be very significant that in some experimental studies β values much below 1/3 and changing abruptly with the acceptor concentration have been encountered.[22] The present simulations make it clear that such values of the β parameter, and their variation with the bulk acceptor concentration, are not consistent with the current view of block copolymer lamella structures. Technical and experimental difficulties may have been the cause of the experimentally observed crossover. Artifacts such as the effect of acceptor (anthracene) emission at the wavelength at which the donor (phenanthrene) emission is collected may appear as an energy transfer effect under certain experimental conditions. The KB analysis of such fluorescence decay curves would lead to unrealistic apparent dimensions. Another, more interesting possibility is that lamellar block copolymer geometry is more "restricted" than implied by the Helfand−Tagami (HT) model. In this case, the difficulties experienced in explaining experimental fluorescence decay curves in terms of HT theory may have been caused by some distribution of junctions *perpendicular* to the axis of the assumed planar symmetry.[34] Block copolymer theory and molecular simulations may shed more light on the latter conjecture.

Conclusions

The simulation of fluorescence decay curves according to the Helfand−Tagami theory for polymer interfaces[27] and the distribution model of energy transfer,[21,23,24,26] allowed us to examine the significance of the apparent dimensions that may be obtained by KB analysis (eq 2). The results conform to an asymptotic theory of HT block copolymers: apparent dimensions approach 3 for broad interfaces but decrease to near 2 for narrow interfaces. From our analysis we found almost perfect proportionality between the P parameter of the intensity function, eq 2, and the acceptor concentration, as well as linear or near linear relationships between apparent dimensions d and the bulk acceptor concentrations. These conclusions appear to be reasonable and can be interpreted in terms of the distribution of donor and acceptor molecules at the interface. The simulation results have also revealed, at least partially, why eq 2 is so successful when applied to lamellar block copolymers.

Nevertheless, the asymptotic formulas and simulation results reported here are in conflict with experimental studies,[10,11,22] where much lower apparent dimensions were found. This conflict can be caused by technical problems in the experimental determination of the decay curves, or by an oversimplification[34] of the junction distribution as described by the Helfand−Tagami theory.[27] If the interface cannot be adequately represented by the assumption of complete planar symmetry, the geometry of the lamellar film would be more "restricted", and the apparent dimension recovered from eq 2 correspondingly lower.

Acknowledgment. The authors thank NSERC Canada for their support of this research. Many of the simulation and analysis techniques employed in this work had been developed earlier in studies supported by the Ontario Centre for Materials Research (now Materials and Manufacturing Ontario, MMO), 3M, 3M Canada, and NSERC Canada. J.P.S. Farinha acknowledges the support of FCT, Project PRAXIS/P/QUI/14057/1998.

Appendix A

Although the concept of an infinitely broad lamellar block copolymer junction is rather nebulous, it is possible to show fairly rigorously that if we let the interface thickness increase without bound in an Helfand−Tagami (HT) model represented by eq 5, we obtain a fluorescence decay formula for junction-labeled block copolymers that is similar to Förster's expression for an isotropic mixture of donors and acceptors in an infinite, three-dimensional volume.

We shall start with the HT junction distribution eq 5, which we normalize using

$$C_D(z) = \frac{2\overline{C_D}}{\pi}\mathrm{sech}\left(\frac{2z}{\delta}\right) \tag{A1a}$$

$$C_A(z) = \frac{2\overline{C_A}}{\pi}\mathrm{sech}\left(\frac{2z}{\delta}\right) \tag{A1b}$$

so that

$$\int_{-\infty}^{\infty} C_D(z)\mathrm{d}z = \delta\overline{C_D} \tag{A2a}$$

$$\int_{-\infty}^{\infty} C_A(z)\mathrm{d}z = \delta\overline{C_A} \tag{A2b}$$

That is, no matter how broad the block copolymer junctions may be, the number of donors and acceptors "per nm^3 of interface" will remain $\overline{C_D}$ and $\overline{C_A}$, respectively. This is analogous to the normalizations in eq 7, for the case where the lamellar period H happens to equal 2δ.

Let us consider a block copolymer film of unit cross section. The radiation emanating from it (cf. eq 4) will be given by

$$I_D(t) = B\exp(-t/\tau_D)\int_{-\infty}^{\infty} C_D(z)\psi(z,t)\,\mathrm{d}z \tag{A3}$$

$$\psi(z,t) = \exp\left\{-2\pi\int_0^{\infty} r\left\{1-\exp\left[-\left(\frac{t}{\tau_D}\right)\left(\frac{R_0^*}{r}\right)^6\right]\right\}\int_{z-r}^{z+r} C_A(z')dz'\,\mathrm{d}r\right\} \tag{A4}$$

where B is an appropriate constant of proportionality or normalizing factor and R_0^* is the Förster radius adjusted for the dipole orientation factor: $(1.5\kappa^2)^{1/6}R_0$.

Since we are seeking an asymptotic formula for very broad interfaces, we will attempt to compute the intensity per unit width: $I_D(t)/\delta$, and then take the limit as $\delta \to \infty$. That is, we wish to find

$$\lim_{\delta\to\infty}\frac{I_D(t)}{\delta} = B\exp(-t/\tau_D)\lim_{\delta\to\infty}\int_{-\infty}^{\infty}\frac{C_D(z)}{\delta}\psi(z,t)\,\mathrm{d}z \tag{A5}$$

We note from eq A1a that $\int_{-\infty}^{\infty} C_D(z)/\delta\,\mathrm{d}z$ is convergent, and since $\psi(z,t)$ is a negative exponential, it immediately follows that the improper integral in eq A5 is *uniformly convergent* with respect to δ. Therefore, when computing the limiting form ($\delta \to \infty$), we may move the limiting process *inside* the integral sign. Furthermore, anticipating that $\lim_{\delta\to\infty}\psi(z,t)$ will not depend on z, we may evaluate eq A5 in a manner reminiscent of the Cauchy principal value:

$$\lim_{\delta\to\infty}\frac{I_D(t)}{\delta} = B\exp(-t/\tau_D)\left[\lim_{\delta\to\infty}\psi(z,t)\right]\lim_{\delta\to\infty}\int_{-\delta}^{\delta}\frac{C_D(z)}{\delta}\mathrm{d}z \tag{A6}$$

The integral shown in eq A6 is, in fact, a finite constant that does not depend on δ. Also, $\psi(z,0)$ equals 1 for any δ (from eq A4 as well as from the physical meaning of $\psi(z,t)$). So, we can complete the normalization to unit intensity at zero time, and obtain

$$\lim_{\delta\to\infty}\frac{I_D(t)}{\delta} = \exp(-t/\tau_D)\lim_{\delta\to\infty}\psi(z,t) \tag{A7}$$

To proceed, we need to examine more closely the *local survival probability function*[23] $\psi(z,t)$ — or its negative logarithm:

$$-\ln[\psi(z,t)] = 2\pi\int_0^\infty r\left\{1-\exp\left[-\left(\frac{t}{\tau_D}\right)\left(\frac{R_0^*}{r}\right)^6\right]\right\}\int_{z-r}^{z+r}C_A(z')dz'\,dr \tag{A8}$$

Only the "inner" integral depends on δ directly; it may be written as

$$\int_{z-r}^{z+r}C_A(z')dz' = \frac{\delta\overline{C_A}}{\pi}\int_{2(z-r)/\delta}^{2(z+r)/\delta}\mathrm{sech}\,u\,du \tag{A9}$$

and it can be shown (by l'Hospital's rule) that its limit as $\delta\to\infty$ is $4r\overline{C_A}/\pi$. Here, we will not attempt to show rigorously that the improper integral of eq A8 is uniformly convergent with respect to δ, but the conjecture is made plausible by the fact that

$$\int_0^\infty r^k\left\{1-\exp\left[-\left(\frac{t}{\tau_D}\right)\left(\frac{R_0^*}{r}\right)^6\right]\right\}dr$$

is convergent even for $k = 3$ or $k = 4$. So, it does seem appropriate to evaluate the limit of the "inner" integral first. Thus, we obtain

$$\lim_{\delta\to\infty}\{-\ln[\phi(z,t)]\} = 8\overline{C_A}\int_0^\infty r^2\left\{1-\exp\left[-\left(\frac{t}{\tau_D}\right)\left(\frac{R_0^*}{r}\right)^6\right]\right\}dr = \frac{8\overline{C_A}R_0^{*3}\pi^{1/2}}{3}\left(\frac{t}{\tau_D}\right)^{1/2} \tag{A10}$$

And finally, combining eqs A7 and A10 yields

$$\lim_{\delta\to\infty}\frac{I_D(t)}{\delta} = \exp\left(-\frac{t}{\tau_D}-\frac{8\overline{C_A}R_0^{*3}\pi^{1/2}}{3}\left(\frac{t}{\tau_D}\right)^{1/2}\right) \tag{A11}$$

The latter formula is very similar to Förster's expression for an isotropic mixture of donors and acceptors in an infinite, three-dimensional volume.[12−14,23] It suggests that when the interface is broad, junction-labeled block copolymers will exhibit fluorescence decay conforming to eq 2, with β approaching 0.5.

Appendix B

The global analysis procedures followed were quite straightforward, except perhaps the way we dealt with the preexponential factor(s). As is customary in time-resolved fluorescence decay studies, we approximated the convolution integral for the delta-function excitation decay curves and a pump pulse by the compound trapezoidal formula. Thus, the "theoretical" fluorescence intensities for channel i (time $i\Delta t$, where Δt is the time scale, ns/channel) and the m-th acceptor concentration in a series of simulations, for a particular junction width, are given by

$$F^0(i,m) = A_m\Delta t\left\{\sum_{j=1}^{i-1}L[(i-j)\Delta t]\exp\left[-\frac{j\Delta t}{\tau_D}-k_1\overline{C_{A,m}}\left(\frac{j\Delta t}{\tau_D}\right)^{\beta_0+k_2\overline{C_{A,m}}}\right]+0.5L(i\Delta t)\right\} \tag{B1}$$

where A_m is a normalizing constant, chosen to yield a theoretical intensity of 20000 counts in the channel of maximum intensity, $L(t)$ is the pump pulse (counts at time t), $\overline{C_{A,m}}$ is the m-th bulk acceptor concentration, and the other model parameters are as in eq 10. The actual [simulated] decay curves to which we fit eq 10 are obtained from eq B1 by adding Poisson noise to each channel. If we now denote the simulated intensity functions by $F(i,m)$ ($F(i,m) = F^0(i,m)$ + noise), then for each channel and each acceptor concentration we wish to define weighted residuals as

$$R(i,m) = \left[F(i,m)-\mathbf{A}\Delta t\left\{\sum_{j=1}^{i-1}L[(i-j)\Delta t]\times\exp\left[-\frac{j\Delta t}{\tau_D}-k_1\overline{C_{A,m}}\left(\frac{j\Delta t}{\tau_D}\right)^{\beta_0+k_2\overline{C_{A,m}}}\right]+0.5L(i\Delta t)\right\}\right]/[F(i,m)]^{1/2} \tag{B2}$$

where **A** denotes a common preexponential factor and $[F(i,m)]^{1/2}$ is the standard deviation associated with a photon count of $F(i,m)$.

The difficulty lies in the circumstance that whereas we have justified that k_1, β_0 and k_2 should be common for the different acceptor concentrations, a priori, one would not expect that the normalizing factors will also be similar for these different simulations. We have resolved this difficulty by adjusting the lamp intensities $L(t)$ employed in the convolutions of eq B2. Specifically, when computing $R(i,m)$, we multiplied the real lamp intensities for each channel by a factor $A_{old}/0.5$, where A_{old} was the preexponential factor recovered when fitting the decay curve representing *only the m-th acceptor concentration* with eq 2. It was now likely that a single normalizing factor **A**, approximately equal to 0.5, would provide good fits to the entire set of simulated fluorescence decay curves (based on all the different acceptor concentrations), provided our assumptions concerning the linear dependence of P and β of eq 2 on $\overline{C_A}$ were reasonable.

Employing the residual formula(s) obtained in the above manner, least-squares fittings were conducted with the Levenberg−Marquardt procedure, as implemented by Moré et al.[32]

Appendix C

We will give brief derivations here of the fluorescence decay functions that arise when the acceptor distributions are described by the Helfand−Tagami model (eqs 5 and 7a), but the donors are all at the center of the interfacial region of a lamella ($z = 0$) or all at $z = \delta$, i.e., at distance δ to the right from the center. This means that eqs 4b to 4d are not affected by the change, but in eq 4a $C_D(z)$ becomes

$$C_D(z) = \frac{H\overline{C_D}}{2}\theta(z) \tag{C1a}$$

or

$$C_D(z) = \frac{H\overline{C_D}}{2}\theta(z-\delta) \tag{C1b}$$

for the centered and off-center donors, respectively, where $\theta(z)$ is the Dirac delta function. (We are denoting it with $\theta(z)$ instead of the more usual $\delta(z)$ notation, since the symbol δ is "reserved" in this paper for Helfand and Tagami's interface thickness parameter, eq 6.)[27] The consequence of this is that the

fluorescence decay functions simplify to

$$\Phi(t) = \exp(-t/\tau_D)\psi(0,t) \quad \text{(C2a)}$$

and

$$\Phi(t) = \exp(-t/\tau_D)\psi(\delta,t) \quad \text{(C2b)}$$

Substituting eqs 4b to 4d, 5 and 7a into the preceding two formulas, introducing dimensionless variables $\rho = r/R_0^*$, $\zeta = 2z/\delta$, and employing the inverse tangent formula[35] for integrating the hyperbolic secant function, we readily obtain the fluorescence decay functions

$$\Phi(t) = \exp\left\{-t/\tau_D - 2H\overline{C_A}R_0^{*2}\int_0^\infty\left[1 - \exp\left(-\frac{t}{\tau_D}\rho^{-6}\right)\right]\left\{2\arctan\left[\exp\left(\frac{2R_0^*\rho}{\delta}\right)\right] - \frac{\pi}{2}\right\}\rho\, d\rho\right\} \quad \text{(C3a)}$$

for donors at the center, and

$$\Phi(t) = \exp\left\{-t/\tau_D - 2H\overline{C_A}R_0^{*2} \times \int_0^\infty\left[1 - \exp\left(-\frac{t}{\tau_D}\rho^{-6}\right)\right]\left\{\arctan\left[\exp\left(2 + \frac{2R_0^*\rho}{\delta}\right)\right] - \arctan\left[\exp\left(2 - \frac{2R_0^*\rho}{\delta}\right)\right]\right\}\rho\, d\rho\right\} \quad \text{(C3b)}$$

for donors at $z = \delta$.

References and Notes

(1) Paul, D. R., Newman, S., Eds. *Polymer Blends*; Academic Press: San Diego, 1978.
(2) Fredrickson, G. H.; Helfand, E. *J. Chem. Phys.* **1987**, *87*, 697.
(3) Bates, F. S.; Fredrickson, G. H. *Annu. Rev. Phys. Chem.* **1990**, *41*, 525.
(4) Stamm, M.; Schubert, D. W. *Annu. Rev. Mater. Sci*. **1995**, *25*, 325.
(5) Russel, T. P. *Phys. B* **1996**, *221*, 267.
(6) Russell, T. P. *MRS Bull.* **1996**, *21*, 49.
(7) Schubert, D. W.; Stamm, M. *Phys. B* **1997**, *234*−*236*, 286.
(8) Sferrazza, M.; Xiao, C.; Jones, R. A. L.; Bucknall, D. G.; Webster, J.; Penfold, J. *Phys. Rev. Lett.* **1997**, *78*, 3693.
(9) Fredrickson, G. H. *Macromolecules* **1986**, *19*, 441.
(10) Ni, S.; Zhang, P.; Wang, Y.; Winnik, M. A. *Macromolecules* **1994**, *27*, 5742.
(11) Tcherkasskaya, O.; Ni, S.; Winnik, M. A. *Macromolecules* **1996**, *29*, 610.
(12) Förster, Th. *Ann. Phys. (Leipzig)* **1948**, *2*, 55.
(13) Förster, Th. *Z. Naturforsch.* **1949**, *4a*, 321.
(14) Baumann, J.; Fayer, M. D. *J. Chem. Phys.* **1986**, *85*, 4087.
(15) Klafter, J.; Blumen, A. *J. Chem. Phys.* **1984**, *80*, 875.
(16) Hauser, M.; Klein, U. K. A.; Gösele, U. Z. *Z. Phys. Chem.* **1976**, *101*, S255.
(17) Blumen, A.; Klafter, J.; Zumofen G. *J. Chem. Phys.* **1986**, *84*, 1397.
(18) Yang, C. L.; Evesque, P.; El-Sayed, M. A. *J. Phys. Chem.* **1985**, *89*, 3442.
(19) Levitz, P.; Drake, J. M.; Klafter, J. In *Molecular Dynamics in Restricted Geometries*; Klafter, J., Drake, J. M., Eds.; John Wiley and Sons: New York, 1989; pp 165−195.
(20) Mataga, N. In *Molecular Dynamics in Restricted Geometries*; Klafter, J., Drake, J. M., Eds.; John Wiley and Sons: New York, 1989; pp 23−37.
(21) Farinha, J. P. S.; Schillén, K.; Winnik, M. A. *J. Phys. Chem. B,* **1999**, *103*, 2487.
(22) Tcherkasskaya, O.; Spiro, J. G.; Ni, S.; Winnik, M. A. *J. Phys. Chem.* **1996**, *100*, 7114.
(23) Yekta, A.; Duhamel, J.; Winnik, M. A. *Chem. Phys. Lett.* **1995**, *235*, 119.
(24) Farinha, J. P. S.; Martinho, J. M. G.; Yekta, A.; Winnik, M. A. *Macromolecules* **1995**, *28*, 6084.
(25) Yekta, A.; Winnik, M. A.; Farinha, J. P. S.; Martinho, J. M. G. *J. Phys. Chem.* **1997**, *101*, 1787.
(26) Farinha, J. P. S.; Martinho, J. M. G.; Kawaguchi, S.; Yekta, A.; Winnik, M. A. *J. Phys. Chem.* **1996**, *100*, 12552.
(27) Helfand, E.; Tagami, Y. *J. Chem. Phys*. **1972**, *56*, 3592.
(28) Yekta, A.; Spiro, J. G.; Winnik, M. A. *J. Phys. Chem. B* **1998**, *102*, 7960.
(29) Even, U.; Rademann, K.; Jortner, J. *Phys. Rev. Lett.* **1984**, *52*, 2164.
(30) Grinvald, A.; Steinberg, I. Z. *Anal. Biochem.* **1974**, *59*, 583.
(31) Beechem, J. M.; Gratton, E.; Ameloot, M.; Knutson, J. R.; Brand, L. In *Topics in Fluorescence Spectroscopy*; Lakowicz, J. R., Editor; Plenum Press: New York, 1991; Vol. 2, pp 241−305.
(32) Garbow, B. S.; Hillstrom, K. E.; Moré, J. J. *Documentation for MINPACK Subroutine LMSTR. Double Precision Version;* Argonne National Laboratory: Argonne, IL, 1980.
(33) Bevington, P. R. *Data Reduction and Error Analysis for the Physical Sciences;* McGraw-Hill: New York, 1969.
(34) Blumen, A.; Personal communication, 1996.
(35) Gradshteyn, I. S.; Ryzhik, I. M. *Table of Integrals, Series and Products*, 5th ed.; Academic Press: Boston, 1994; p 51.